

Filtered Back Projection, Adaptive Statistical Iterative Reconstruction, and a Model-based Iterative Reconstruction in Abdominal CT: An Experimental Clinical Study¹

Zsuzsanna Deák, MD
Jochen M. Grimm, MD
Marcus Treitl, MD
Lucas L. Geyer, MD
Ulrich Linsenmaier, MD
Markus Körner, MD
Maximilian F. Reiser, MD
Stefan Wirth, PhD, MD

Purpose:

To compare objective and subjective image quality parameters of three image reconstruction algorithms of different generations at routine multidetector computed tomographic (CT) examinations of the abdomen.

Materials and Methods:

This institutional review board–approved study included 22 consecutive patients (mean age, 56.1 years \pm 15.8 [standard deviation]; mean weight, 79.1 kg \pm 14.8) who underwent routine CT examinations of the abdomen. A low-contrast phantom was used for objective quality control. Raw data sets were reconstructed by using filtered back projection (FBP), adaptive statistical iterative reconstruction (ASIR), and a model-based iterative reconstruction (MBIR). Radiologists used a semiquantitative scale (–3 to +3) to rate subjective image quality and artifacts, comparing both FBP and MBIR images with ASIR images. The Wilcoxon test and the intraclass correlation coefficient were used to evaluate the data. Measurements of objective noise and CT numbers of soft tissue structures were compared with analysis of variance.

Results:

The phantom study revealed an improved detectability of low-contrast targets for MBIR compared with ASIR or FBP. Subjective ratings showed higher image quality for MBIR, with better resolution (median value, 2; range, 1 to 3), lower noise (2; range, 1 to 3), and finer contours (2; range, 1 to 2) compared with ASIR (all $P < .001$). FBP performed inferiorly (0, range, –2 to 0); –1 [range, –3 to 0]; 0 [range, –1 to 0], respectively; all, $P < .001$). Mean interobserver correlation was 0.9 for image perception and 0.7 for artifacts. Objective noise for FBP was 14%–68% higher and for MBIR was 18%–47% lower than that for ASIR ($P < .001$).

Conclusion:

The MBIR algorithm considerably improved objective and subjective image quality parameters of routine abdominal multidetector CT images compared with those of ASIR and FBP.

©RSNA, 2012

¹From the Department for Clinical Radiology, Ludwig-Maximilians-University, Campus Innenstadt, Nussbaumstrasse 20, 80336 Munich, Germany. Received December 20, 2011; revision requested February 3, 2012; revision received May 17; accepted June 8; final version accepted July 24. Address correspondence to Z.D. (e-mail: zsuzsanna.deak@med.uni-muenchen.de).

Multidetector computed tomography (CT) is well established and its use in clinical routine continues to grow. However, this increased use has led to substantial concerns about patient exposure to radiation (1–3). Consequently, recent technical developments have included the introduction of image reconstruction algorithms that improve and optimize data processing to allow for radiation dose reduction while maintaining diagnostic image quality (4–7). The filtered back projection (FBP) algorithm, an analytic approach of image reconstruction, has been the standard method for a long time.

Since 2009, manufacturers have adapted several types of iterative reconstruction algorithms for use in CT, including iterative reconstruction in image space (8,9), adaptive iterative dose

reduction (10), adaptive statistical iterative reconstruction (ASIR) (11–16), sonogram-affirmed iterative reconstruction (17,18) and iDOSE (19–22), to allow a decrease in radiation exposure.

These iteratively enhanced algorithms have in common the application of a predictor model of statistical noise supported by the noise propagation of the image domain. These algorithms are reported to allow for a dose reduction of 29%–66% at abdominal multidetector CT and have been accepted as feasible and standard reconstruction algorithms in clinical routine. To our knowledge, comparative clinical studies of this commercial software have not been published yet. However, several reports exist on the dose reduction potential of these methods in clinical routine examinations (6–20).

Recently, a fully iterative algorithm, the model-based iterative reconstruction (MBIR) algorithm, became available. In addition to allowing calculation of noise statistics, MBIR uses a more complex system of prediction models, which includes modeling of optical factors such as x-ray tube response, detector response, and many other aspects of x-ray physics (eg, scatter, crosstalk), and exact geometric features of the cone beam and the absorbing voxels (7, 23). Phantom studies revealed initially promising results for MBIR, but clinical studies are, to our knowledge, not yet available (22–25).

The purpose of this study was to compare objective and subjective image quality parameters of three image reconstruction algorithms of different generations on images from routine multidetector CT examinations of the abdomen.

Materials and Methods

GE Healthcare (Waukesha, Wis) provided the hardware and software support

Implication for Patient Care

- Although MBIR is a reliable and safe method to help reduce radiation dose at CT, current high reconstruction time limits its benefits to nonemergency cases.

for the reconstruction of MBIR images. Z.D. received a research grant from GE Healthcare from September 2010 to August 2011 and M.K. was a consultant for GE Healthcare from September 2009 to December 2011. All other authors had control of inclusion of any data and information that might present a conflict of interest. Good clinical practice and the Declaration of Helsinki were strictly followed. A waiver of consent was granted by the local ethics committee and the institutional scientific review board.

Patients and Study Design

Twenty-two consecutive patients (55% men; mean age, 56.1 years \pm 15.8 [standard deviation]; mean age of men, 55.0 years \pm 15.6; of women, 57.2 years \pm 14.5; mean patient weight, 79.1 kg \pm 14.8) who underwent standard-of-care multidetector CT examinations of the abdomen (CT dose index, 9.1 mGy \pm 4.1; dose-length product, 476 mGy/cm \pm 219) were enrolled in this single-center study. Raw data sets of these patients were retrospectively extracted and processed to prospectively compare the three different reconstruction algorithms.

CT System Parameters

Images were obtained by using a 64-row multidetector CT scanner (HD 750 Discovery; GE Healthcare) with a

Advances in Knowledge

- Use of model-based iterative reconstruction (MBIR) algorithm decreased image noise by up to 47% compared with adaptive statistical iterative reconstruction (ASIR) and 58% compared with noniterative filtered back projection (FBP) algorithms.
- Use of MBIR significantly improved subjective image quality compared with that of both the ASIR ($P < .001$) and the FBP ($P < .001$) methods. The algorithm-associated new artifacts had little effect on this quality improvement.
- The evaluation of low-contrast target detection revealed that targets with 0.5% nominal contrast levels were detectable in areas as small as 7 mm in diameter on MBIR images at 40 mAs, whereas the same targets were identifiable on ASIR and FBP images only at 120 and 240 mAs, respectively.
- The reconstruction of MBIR images required increased computational power and an extended reconstruction time of 15 to 30 minutes for a single scan.

Published online before print

10.1148/radiol.12112707 **Content codes:**  

Radiology 2013; 266:197–206

Abbreviations:

ASIR = adaptive statistical iterative reconstruction

FBP = filtered back projection

MBIR = model-based iterative reconstruction

Author contributions:

Guarantors of integrity of entire study, Z.D., M.T., U.L., S.W.; study concepts/study design or data acquisition or data analysis/interpretation, all authors; manuscript drafting or manuscript revision for important intellectual content, all authors; approval of final version of submitted manuscript, all authors; literature research, Z.D., M.T., M.F.R., S.W.; clinical studies, Z.D., L.L.G., U.L., S.W.; experimental studies, Z.D., J.M.G., U.L., M.K., S.W.; statistical analysis, Z.D., M.T., M.K., S.W.; and manuscript editing, Z.D., J.M.G., M.T., U.L., M.K., M.F.R., S.W.

Conflicts of interest are listed at the end of this article.

fixed delay of 65 seconds after aortal bolus tracking. The threshold was set at 150 HU. All patients received 450 mg per kilogram of iodinated contrast medium (Solustrast 300; Bracco Imaging Deutschland, Konstanz, Germany) at an injection rate of 3.5 mL per second and 1500 mL of a 1:100 diluted oral contrast medium (300 mg of iodine per mL, Peritragst GI; Dr. Franz Köhler Chemie, Bensheim, Germany). Scan parameters were detector collimation, 0.625 mm; tube voltage, 120 kV; rotation time, 0.4 sec; z-axis modulated tube current, 100–600 mA (40–240 mAs tube current-time product); noise index, 43. ASIR was performed by using a blending level of 50% on the basis of our own prior results and the maker's recommendation for image reconstruction in section mode (26).

Phantom Study

A CATPHAN600 phantom (The Phantom Laboratory, Greenwich, NY) was included in this study for quality control. The cylindrical phantom allows for an objective determination of low-contrast resolution. It contains 3×9 low-contrast targets representing three different contrast levels (1.0%, 0.5%, and 0.3%). Each series of the nine targets featured varying diameters (2–9 mm and 15 mm). The 15-mm target usually serves for contrast-to-noise ratios; the other eight targets were used for low-contrast detection.

In the first part of the phantom study, the phantom was positioned in three perpendicular orientations to help assess the detectability of low-contrast targets in all three imaging planes by using the routine abdominal multidetector CT protocol with fixed milliamperere setting of 600 mA (240 mAs, CT dose index, 16.2 mGy). All imaging was performed by using the same CT scanner. In the second part of the phantom study, we added five more incrementally decreasing fixed tube current steps (100 mA/40 mAs, 200 mA/80 mAs, 300 mA/120 mAs, 400 mA/160 mAs, 500 mA/200 mAs; CT dose index: 2.7 mGy, 5.4 mGy, 8.1 mGy, 10.8 mGy, 13.5 mGy, respectively) without changing the other scan parameters to evaluate low-contrast

resolution at decreasing radiation doses in the axial plane.

Image Reconstruction

Raw data were reconstructed by using axial sections of 0.625-mm images with the standard soft tissue kernel and (a) ASIR at 50% in section mode, (b) FBP, and (c) MBIR (Veo; GE Healthcare). Thin-section data were reformatted by using a section thickness of 5 mm. Phantom data were identically processed (soft tissue kernel; section thickness of reconstructed and reformatted images, 0.625 mm and 5 mm, respectively; reconstruction algorithms, ASIR at 50% in section mode, FBP, MBIR).

Analysis of Image Quality

The studies were evaluated on the same workstation (Advantage Workstation, GE Healthcare). Displays were calibrated and all viewing conditions were held constant according to the applicable recommendations (American Association of Physics in Medicine Task Group 18 report [27]).

Evaluation of subjective image quality.—The noise index of the scan protocols was optimized for ASIR, and subjective image quality was evaluated by comparing MBIR and FBP images to ASIR images. FBP and MBIR scan series of different imaging planes were presented randomly to three blinded radiologists (J.M.G., M.T., S.W. with 3–10 years of experience in CT) and were compared with the corresponding ASIR series. Subjective image quality assessment of different anatomic structures was based on accepted standards (European Diagnostic Guidelines for Quality Criteria [28]).

FBP and MBIR reformation series were presented randomly to three blinded radiologists (J.M.G., M.T., S.W.). Each reformatted image series was compared with the corresponding ASIR reformation in pairs so that one single reformation (eg, all axial images of one patient) of MBIR or FBP reconstructions was presented on the right screen and the identical ASIR reformation was on the left screen. Subjective image quality assessment

of different anatomic structures was based on established standards (European Diagnostic Guidelines for Quality Criteria [29]).

Each reformation was selectively evaluated. Readers independently and selectively assessed all reformations one by one, taking into consideration three quality aspects: image noise, resolution, and the contours of the different soft tissue interfaces. A semiquantitative seven-point scale (from –3 for inferior [impairing diagnosis] to +3, for superior [easing diagnosis]; –2 for inferior [probably impairing diagnosis] to +2 for superior [probably easing diagnosis]; –1 for slightly inferior (no influence on diagnosis] to +1 slightly superior [no influence on diagnosis]; and 0, equal) was used. In this evaluation process the corresponding ASIR images were the control images, with a nominal value of 0 on the –3 to +3 scale. Mean image quality scores were calculated individually for each of the three readers and separately for each image plane. Median values of image quality scores assigned by each reader to every aspect on every plane were recorded separately. From scores of all readers, an overall median image quality score was calculated for each aspect in each plane (Table 1).

Evaluation of image artifacts.—Image artifacts were characterized as differences between the expected attenuation values of an object and the actual measured HU. Artifacts (mainly streaking) due to beam hardening and photon starvation can often seriously impair image quality in abdominal CT (30). Newer methods of image reconstruction may produce image artifacts that were previously not recorded. However, artifacts associated with partially iterative reconstruction algorithms have not yet been reported (to our knowledge), but MBIR, being a full iterative algorithm representing a completely different reconstruction approach, is less known and less evaluated in the clinical routine (31). Consequently, we recognized and subjectively analyzed the possibility of previously unrecorded image artifacts by rating subjective image quality with the methods that we have described in this article.

Table 1

Subjective Image Quality and Artifacts

Imaging Perceptions and Artifacts by Imaging Plane	FBP						MBIR						MBIR vs ASIR P Value	ICC P < .001	
	Median			Range			Median			Range					
	R1	R2	R3	All	Min	Max	R1	R2	R3	All	Min	Max			
Imaging perception															
Axial															
Resolution	0	0	0	0	-1	0	<.001*	2	2	2	2	1	3	<.001*	0.917
Noise	-1	-1	-1	-1	-3	0	<.001*	2	2	2	2	1	3	<.001*	0.804
Contour	0	0	0	0	-1	0	.156	2	1	2	2	1	2	<.001*	0.880
Sagittal															
Resolution	0	0	0	0	-1	0	.610	2	2	2	2	1	2	<.001*	0.905
Noise	0	-1	-1	-1	-2	0	<.001*	2	2	2	2	1	2	<.001*	0.900
Contour	0	0	0	0	0	0	.317	2	1	2	2	1	2	<.001*	0.808
Coronal															
Resolution	0	0	0	0	-2	0	.230	2	2	2	2	1	2	<.001*	0.922
Noise	0	-1	-1	-1	-2	0	<.001*	2	2	2	2	1	2	<.001*	0.904
Contour	0	0	0	0	0	0	.99	2	1	2	2	1	2	<.001*	0.830
Artifacts															
Axial															
Beam hardening	0	0	0	0	-1	0	<.001*	1	1	1	1	0	3	<.001*	0.663
Photon starvation	0	0	0	0	-1	0	<.001*	1	2	1	1	0	3	<.001*	0.650
Staircase	0	0	0	0	0	0	.99	-1	-1	-1	-1	-2	0	<.001*	0.880
Dark border	0	0	0	0	0	0	.99	-1	-2	-1	-1	-2	0	<.001*	0.905
Sagittal															
Beam hardening	0	-1	0	0	-1	0	<.001*	1	1	1	1	0	3	<.001*	0.671
Photon starvation	0	0	0	0	-1	0	.001*	1	2	1	1	0	3	<.001*	0.650
Staircase	0	0	0	0	0	0	.99	-1	-1	-1	-1	-2	0	<.001*	0.880
Dark border	0	0	0	0	0	0	.99	0	-1	0	0	-2	0	<.001*	0.549
Coronal															
Beam hardening	0	-1	0	0	-1	0	<.001*	1	1	1	1	0	3	<.001*	0.652
Photon starvation	0	0	0	0	-1	0	.001*	1	1	1	1	0	3	<.001*	0.661
Staircase	0	0	0	0	0	0	.000*	0	-1	-1	-1	-2	0	<.001*	0.830
Dark border	0	0	0	0	0	0	.99	0	-1	-1	0	-2	0	<.001*	0.198

Note.—Data are subjective image quality ratings regarding resolution, noise, contour, and artifacts in comparison with baseline ASIR image rating at 0. R = reader.

* P value indicates significant difference.

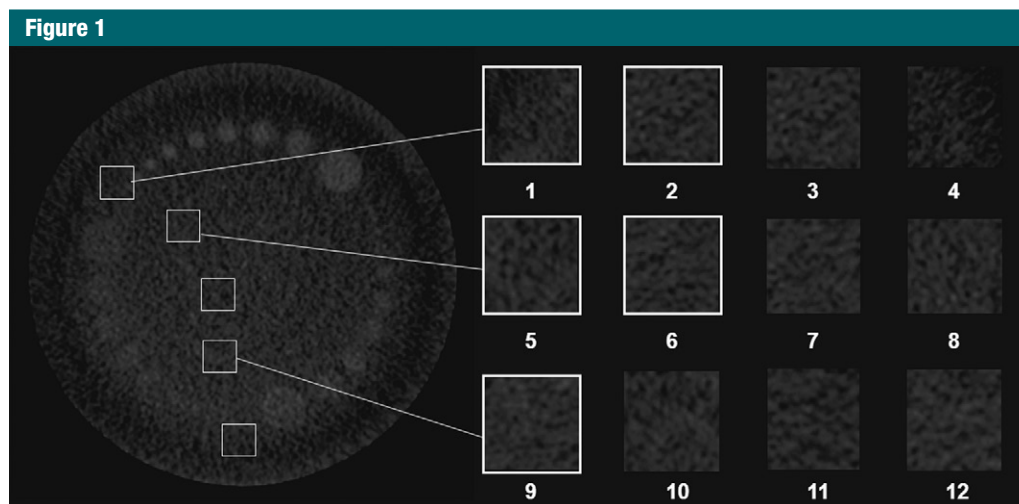


Figure 1: CT image shows modified version of multiple-alternative forced-choice method. In each experiment, 12 numbered squares were presented to observers. Only one square contained signal, and observer chose square most likely to contain signal.

Evaluation of quantitative image quality.—Ten-millimeter circular regions of interest were drawn in representative soft tissue (gluteal fat tissue, liver, and urinary bladder); mean attenuation values and the standard deviation of the mean attenuation values for each region of interest served as objective measurements to estimate image noise. The size and position of each region of interest was kept constant throughout the entire study; three measurements were calculated as mean values for each region of interest in all datasets and all image planes. The mean attenuation values and the values of the standard deviations were analyzed and compared selectively for each soft tissue type and each plane. ASIR served as the common control. Noise levels measured in the standard planes were compared and tested for differences among axial, sagittal, and coronal reformations for each reconstruction method.

Low contrast resolution was defined on detection of the smallest low-contrast targets. A modified version of the multiple-alternative forced-choice method served as the evaluation technique to help avoid potential reader-dependent subjective effects (29). The number of the observers was increased to six (the three radiologists performing the subjective image evaluation and

three additional radiologists who participated only in the phantom study) to increase the accuracy of the low-contrast detection. The six blinded observers located the targets on randomly chosen images. Targets were considered detectable if at least five of the six radiologists independently indicated them as such. The method applied is detailed and demonstrated in Figure 1.

In addition to low-contrast detection, contrast-to-noise ratios were calculated in the 15-mm targets as recommended in the phantom's manual. For every dose step, nine measurements were performed in regions of interest placed in each of the reformatted axial sections.

Statistical Data Analysis

Values of mean attenuation and standard deviation were first tested with the Levene test for homogeneity of distribution and with one-way analysis of variance. The Tukey honestly significant difference test was used as a post hoc test. In cases of inhomogeneous data distribution, the Welch and Games-Howell tests were used. Subjective image ratings were compared with the Wilcoxon test corrected for multiple comparisons according to the Bonferroni adjustment. Interreader reliability was calculated by using the intraclass

correlation coefficient. Software was used for the calculations (Predictive Analytics SoftWare Statistics 18.0.0; IBM, Armonk, NY). A P value of less than .05 was considered to indicate a statistically significant difference, except for Bonferroni-corrected Wilcoxon test P values, for which less than .025 was considered to indicate a significant difference.

Results

Evaluation of Subjective Image Quality and Artifacts

The median values of image quality scores assigned by each reader to every aspect in every plane and the corresponding intraclass correlation coefficients are summarized in Table 1.

Subjective image quality.—Compared with ASIR, more image noise was found on FBP reformations (median scores for all planes, -1) without impaired spatial resolution or affected soft tissue contours in the subjective image evaluation ($P < .001$). Significant differences of spatial resolution between ASIR and FBP were noticed only on axial reformations ($P < .001$). MBIR was superior to ASIR. In all planes, FBP significantly improved resolution (medians for all planes, $+2$), decreased image noise (medians for all

planes, +2) and provided clearer contours (medians for all planes, +2) of soft-tissue interfaces ($P < .001$). The results of the rating scores translated the difference as a significant and major (+2) subjective image quality improvement in favor of MBIR, and the image quality inferiority of FBP compared with ASIR was interpreted as a minor effect (−1) particularly attributable to image noise leading to slightly but detectably decreased spatial resolution on axial images. Intraclass correlation coefficients ranged from 0.804 to 0.922, indicating high agreement among the three readers.

Artifacts.—ASIR and MBIR showed potential to reduce CT artifacts, such as beam hardening and photon starvation, in critical anatomic locations, such as along the spine or in the bony pelvis (Fig 2). MBIR efficiently and significantly reduced photon starvation and beam hardening artifacts in all anatomic planes ($P < .001$). FBP was slightly but significantly inferior to ASIR ($P \leq .001$), although this effect remained less apparent (medians for all planes were 0 for both artifact types).

MBIR images showed a new phenomenon: a subtle staircase effect on bony interfaces, mostly of cortical bone. This alteration of high-contrast structure interfaces could be recognized in all planes and showed a significant ($P < .001$) but minor negative effect on image quality (medians for all planes, −1) in all planes. This staircase effect was consistently recognized (intraclass correlation coefficient, 0.830–0.880).

In the MBIR images, another form of artifact appeared as small blacked-out pixels on skin surfaces. Although the effect on the image quality of this artifact proved to be significant in all planes ($P < .001$), it seemed to have only a minor negative effect on overall image quality, mainly on axial reformations (median for axial, sagittal, and coronal planes, respectively, −1, 0, 0). These bordering blacked-out artifacts typically occurred solely on the interfaces of skin and air (Fig 3) and led to a local loss of potentially diagnostic information. They were present on images from 15 abdominal CT scans of the inguinal region with either a major (−2, axial) or

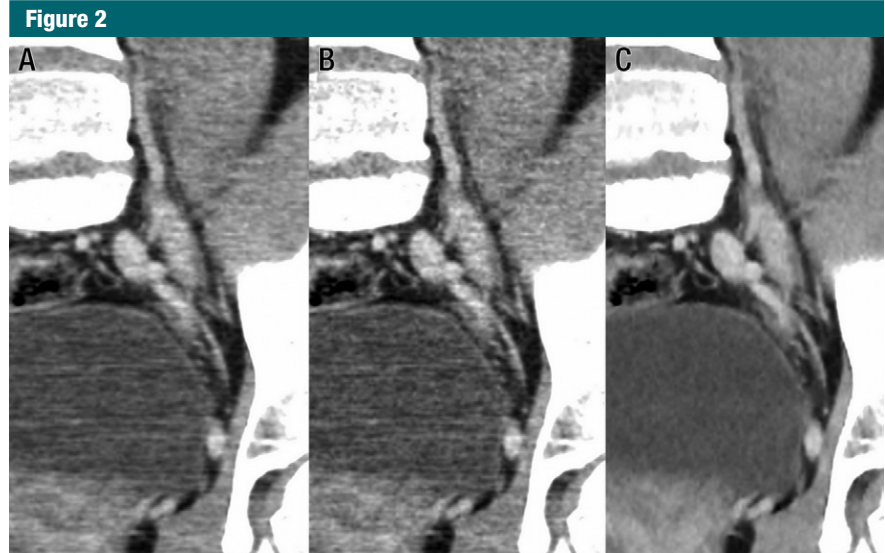


Figure 2: CT images show subjective image quality and artifacts. Image quality of three reconstruction methods is shown: A, ASIR; B, FBP, and C, MBIR. Note subtle staircase artifacts of bony contour of pelvic ring in C.

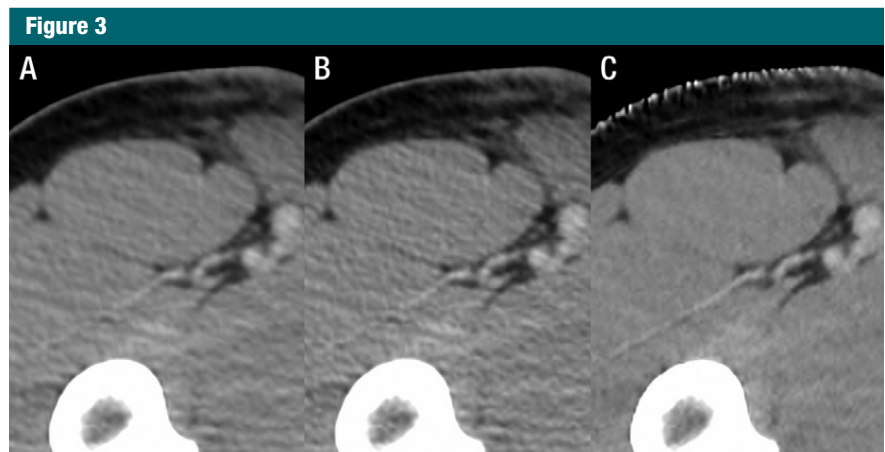


Figure 3: CT images show subjective image quality and artifacts. Images reconstructed with A, ASIR; B, FBP, and C, MBIR. Note dark-bordered artifacts on contact surface of air and skin and improved resolution, improved noise reduction, and fine outlines in C.

minor (−1, sagittal and coronal) negative effect on image quality. The bordering blacked-out artifact mainly impaired the image quality of axial reformations (median, −1). Its effect on image quality on sagittal and coronal reformations was significant but less obvious (median sagittal and coronal, 0) and ratings of the three readers were also less consistent (intraclass correlation coefficient, 0.549–0.198).

Quantitative Image Quality

Objective noise measurements.—The mean attenuation values and image noise level values (mean value of measured standard deviations of attenuation values) are displayed in Tables 2 and 3. Mean attenuation values measured in different soft tissue structures were independent of imaging plane and reconstruction algorithm ($P \geq .98$). Noise levels were significantly different

Table 2

Objective Image Noise

Soft Tissue	FBP			ASIR			MBIR		
	Axial	Sagittal	Coronal	Axial	Sagittal	Coronal	Axial	Sagittal	Coronal
Attenuation (HU)*									
Liver	101.7 ± 17.5	102.0 ± 17.4	101.8 ± 17.4	101.6 ± 17.5	102.2 ± 17.2	102.0 ± 17.2	101.9 ± 17.3	102.0 ± 17.0	102.0 ± 17.2
Fat tissue	-100.1 ± 10.8	-99.5 ± 11.2	-100.1 ± 11.2	-99.9 ± 10.8	-99.9 ± 10.9	-99.8 ± 11.3	-98.1 ± 11.3	-97.4 ± 11.8	-98.1 ± 12.3
Bladder	-1.9 ± 5.4	-1.2 ± 5.9	-1.0 ± 6.3	-1.7 ± 5.6	-1.6 ± 5.9	-1.0 ± 6.2	-0.6 ± 6.4	-0.3 ± 6.5	0.0 ± 6.7
Noise†									
Liver	19.3 ± 3.6	20.6 ± 4.1	15.0 ± 1.7	14.2 ± 2.2	16.0 ± 2.4	12.1 ± 1.1	10.1 ± 1.5	9.1 ± 1.8	8.9 ± 1.3
Fat tissue	16.1 ± 3.7	19.5 ± 4.3	13.0 ± 2.9	12.6 ± 2.4	15.9 ± 3.6	12.3 ± 2.7	9.4 ± 1.5	9.7 ± 4.1	9.2 ± 2.9
Bladder	16.4 ± 3.3	18.5 ± 4.6	13.3 ± 2.6	11.7 ± 2.5	14.6 ± 3.7	10.2 ± 2.3	8.8 ± 1.4	7.7 ± 2.1	7.7 ± 1.7

* Data are means ± standard deviation. No significant differences were found (*P* values of .99 for liver, .993 for fat, .983 for bladder; multiple comparisons test).

† Data are means ± standard deviation. Data were significantly different (*P* values of <.001 for liver, fat, and bladder; multiple comparisons test).

Table 3

Post hoc Test Results

A: Reconstruction Methods

Soft Tissue	FBP vs ASIR			MBIR vs ASIR		
	Axial	Sagittal	Coronal	Axial	Sagittal	Coronal
Liver	<.001*	.003*	<.001*	<.001*	<.001*	<.001*
Fat tissue	.011*	.007*	.99	.038*	<.001*	.035*
Bladder	<.001*	.111	.007*	.001*	<.001*	.008*

B: Imaging Planes

Soft Tissue	FBP			ASIR			MBIR		
	Axial vs Sagittal	Sagittal vs Coronal	Coronal vs Axial	Axial vs Sagittal	Sagittal vs Coronal	Coronal vs Axial	Axial vs Sagittal	Sagittal vs Coronal	Coronal vs Axial
Liver	.974	<.001*	.001*	.246	<.001*	.021*	.572	.99	.197
Fat tissue	.013*	<.001*	.052	.019	.009*	.99	.99	.99	.99
Bladder	.780	.002*	.034*	.101	.002*	.544	.745	.99	.617

Note.—Data are *P* values. All *P* < .05 indicate significant difference.

Table 4

Low-Contrast Resolution of the Reconstruction Methods

Nominal Contrast Percentage	FBP			ASIR			MBIR		
	Axial	Sagittal	Coronal	Axial	Sagittal	Coronal	Axial	Sagittal	Coronal
1.0%	3	5	5	2	5	5	2	3	3
0.5%	7	9	9	3	7	6	3	4	4

Note.—Data are millimeters.

among the images reconstructed with the three algorithms (Table 2). Objective noise was 14%–68% higher for FBP and 18%–47% lower for MBIR

images than it was for ASIR images (*P* < .05). MBIR yielded no significant difference in image noise among all planes (*P* ≥ .20).

Low-contrast resolution in the phantom study.—The low-contrast resolution of the three reconstruction algorithms for the three planes are listed in Table 4. The results of the contrast-to-noise ratios and low-contrast detection for the dose-reduced protocols with consecutive dose reduction steps are summarized in Figure 4. In addition, as a result of the post hoc test, the groups of contrast-to-noise ratio values are displayed in homogeneous subsets in Table 5. Contrast-to-noise ratios of the 1% and 0.5% contrast targets and the results of low-contrast detection experiments show that low-contrast detection

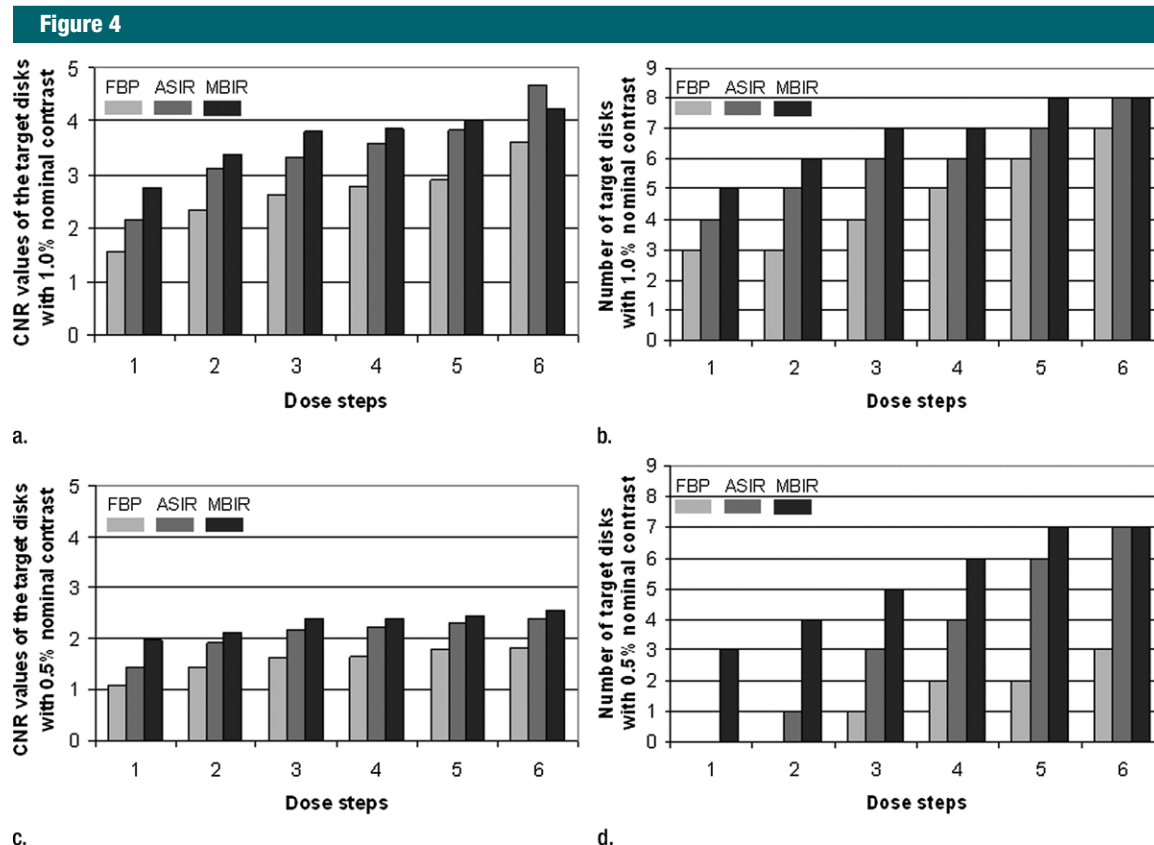


Figure 4: Bar graphs show phantom study data. Columns show mean contrast-to-noise ratios of (a) 1.0% and (c) 0.5% low-contrast targets and numbers of detected (b) 1.0% and (d) 0.5% low-contrast targets. Numbers 1–6 on x axis indicate the six dose steps from 40 mAs to 240 mAs.

of MBIR at 40 mAs is comparable to that of ASIR at 120 mAs and FBP at 240 mAs.

Discussion

To our knowledge, this is the first clinical study in which a fully iterative algorithm was systematically evaluated for image quality and artifacts and compared with those of a partially iterative and analytic method by using the same raw datasets for image reconstruction.

Our results showed that MBIR significantly improves image quality for standard-dose clinical routine imaging compared with that of ASIR. This difference is even more pronounced than the improvement of ASIR compared with FBP. The MBIR algorithm improves low contrast resolution and decreases image noise represented by the standard

deviation of mean attenuation values in homogeneous soft tissues without altering the mean attenuation value.

The results of our phantom study confirm these findings and suggest that use of MBIR could allow for diagnostic image quality at greatly reduced tube currents. This is in accordance with the results of the phantom study of Miéville et al (24). By using the MBIR algorithm, we recorded the appearance of stairstep artifacts of high-contrast structure interfaces and skin-associated bordering blacked-out artifacts, accompanied by a local loss of information. Both artifacts showed minor effects on subjective image quality.

Iterative reconstruction approaches use a predefined noise model based on Poisson counting statistics (ASIR) or a complex system model (MBIR) to refine raw data but require increased

computational capacity. Today, the available computational capacity allows for bearable image processing times, yielding diagnostic images within a few minutes for iteratively enhanced algorithms. The ASIR algorithm, for example, requires only a little more processing time than standard FBP, with an increase of no more than 30%–50%, according to current reports (10,13,14). Data processing of the fully iterative algorithm by using consecutive iterations is far more complex and, despite advanced server technology, reconstruction times for standard thoracic and abdominal CT datasets with 0.625-mm image collimation was about 15–30 minutes for a single scan. This fact limits its clinical applications to nonemergency cases.

The study had several limitations. High contrast resolution was not eval

Table 5
Contrast-to-Noise Ratios at Six Dose Steps

Group-related Lowest P Value	FBP						ASIR						MBIR					
	1	2	3	4	5	6	1	2	3	4	5	6	1	2	3	4	5	6
	1.0% Contrast																	
.99	1.54
>.78	...	2.33	2.61	2.16	2.73
>.84	...	2.33	2.61	2.77	2.90	2.73
>.237	2.77	2.90	3.11	2.73
>.060	2.77	2.90	3.11	3.32	2.73
>.327	2.90	3.11	3.32	3.32	3.37
>.231	3.61	...	3.11	3.32	3.58	3.37
>.182	3.61	3.32	3.58	3.84	3.37	3.80	3.84	4.01	...
>.519	3.61	3.58	3.84	3.80	3.84	4.01	...
>.081	3.84	4.66	3.80	3.84	4.01	4.37
>.961	4.66	4.37
	0.5% Contrast																	
>.603	1.08	1.44	1.43
>.072	1.08	1.44	1.62	1.63	1.43	1.92	1.96
>.088	1.62	1.63	1.80	1.82	...	1.92	1.96	2.13
>.088	1.80	1.82	...	1.92	2.19	2.22	2.31	...	1.96	2.13	2.39
>.072	1.92	2.19	2.22	2.31	2.37	1.96	2.13	2.39	2.40	2.44	...
>.390	2.19	2.22	2.31	2.37	...	2.13	2.39	2.40	2.44	2.54

Note.—Data are mean contrast-to-noise ratios at six dose steps (indicated by column heads 1–6 for tube current products from 40 mAs to 240 mAs) by reconstruction method, displayed in homogeneous subsets. $P < .05$ indicates a statistically significant difference. Mean contrast-to-noise ratios that were not significantly different (ie, $> .05$) appear in the same row. For instance, contrast-to-noise ratios of 1% contrast targets measured in MBIR images at 40 mAs (column 1) are not significantly different from those in ASIR images at 120 mAs (column 3) and in FBP images at 200 mAs (column 5); contrast-to-noise ratios of 0.5% targets in MBIR images at 40 mAs (column 1) are comparable to those in ASIR and FBP images at 240 mAs (column 6).

uated and image quality comparison was not performed on patient data for low-dose CT protocols, but on phantom scans. Lowering the radiation dose below accepted clinical levels that could impair diagnostic quality is ethically as unacceptable as performing multiple dose-reduced scans on the same patient. Furthermore, ratings of the subjective image quality are, by their nature, restricted to subjective impressions of the presented images. Interobserver correlation coefficients were calculated to assess the reliability of the data, and objective measurements were used to indirectly affirm the reliability of the subjective ratings. For example, the evaluation of analogous phantom scans enabled an objective demonstration of the improved spatial resolution of MBIR images for all planes; measurements of standard deviations of CT attenuation values allowed objective determination of image noise levels in addition to the subjective evaluation of image appearance.

In conclusion, our data suggest that MBIR, as a fully iterative method, considerably improved image quality in comparison with both the partially iterative ASIR algorithm and the traditionally applied noniterative FBP. Considering its excellent performance in standard-dose CT protocols and low-dose phantom scans, we believe it is promising for low-dose CT applications. Further studies are required to develop reliable dose-reduced multidetector CT protocols for clinical routine and to systematically analyze the performance of MBIR for detection of various pathologic conditions. However, the long processing time limits its clinical applications to nonemergency cases.

Disclosures of Conflicts of Interest: Z.D. Financial activities related to the present article: none to disclose. Financial activities not related to the present article: Institution received general research grant from GE. Other relationships: none to disclose. J.M.G. Financial activities related to the present article: none to disclose. Financial activities not related to the present article: Institution received general research grant. Author received payment from GE for scientific presentations. Other relationships: none to disclose. M.T. Financial activities related to the present article: none to disclose. Financial activities not related to the present article: Received payment for lectures and consultancy from Ev3 Inc. Other relationships: none to disclose. L.L.G. Financial activities related to the present article: none to disclose. Financial activities not related to the present article: Re-

ceived payment for lectures from GE Healthcare, Germany. Other relationships: none to disclose. **U.L.** Financial activities related to the present article: none to disclose. Financial activities not related to the present article: Institution received payment for lectures and grants from GE. Other relationships: none to disclose. **M.K.** No relevant conflicts of interest to disclose. **M.E.R.** Financial activities related to the present article: none to disclose. Financial activities not related to the present article: Institution received payment for lectures and grants from GE. Other relationships: none to disclose. **S.W.** Financial activities related to the present article: none to disclose. Financial activities not related to the present article: Institution received payment for lectures and grants from GE. Other relationships: none to disclose.

References

- Hall EJ, Brenner DJ. Cancer risks from diagnostic radiology. *Br J Radiol* 2008;81(965):362–378.
- Brenner DJ, Elliston CD. Estimated radiation risks potentially associated with full-body CT screening. *Radiology* 2004;232(3):735–738.
- Mettler FA Jr, Thomadsen BR, Bhargavan M, et al. Medical radiation exposure in the U.S. in 2006: preliminary results. *Health Phys* 2008;95(5):502–507.
- Gunn ML, Kohr JR. State of the art: technologies for computed tomography dose reduction. *Emerg Radiol* 2010;17(3):209–218.
- Thibault JB, Sauer KD, Bouman CA, Hsieh JA. A three-dimensional statistical approach to improved image quality for multislice helical CT. *Med Phys* 2007;34(11):4526–4544.
- Nelson RC, Feuerlein S, Boll DT. New iterative reconstruction techniques for cardiovascular computed tomography: how do they work, and what are the advantages and disadvantages? *J Cardiovasc Comput Tomogr* 2011;5(5):286–292.
- Fleischmann D, Boas FE. Computed tomography—old ideas and new technology. *Eur Radiol* 2011;21(3):510–517.
- Ghetti C, Ortenzia O, Serrelli G. CT iterative reconstruction in image space: a phantom study. *Phys Med* 2012;28(2):161–165.
- May MS, Wüst W, Brand M, et al. Dose reduction in abdominal computed tomography: intraindividual comparison of image quality of full-dose standard and half-dose iterative reconstructions with dual-source computed tomography. *Invest Radiol* 2011;46(7):465–470.
- Gervaise A, Osemont B, Lecocq S, et al. CT image quality improvement using Adaptive Iterative Dose Reduction with wide-volume acquisition on 320-detector CT. *Eur Radiol* 2012;22(2):295–301.
- Silva AC, Lawder HJ, Hara A, Kujak J, Pavlicek W. Innovations in CT dose reduction strategy: application of the adaptive statistical iterative reconstruction algorithm. *AJR Am J Roentgenol* 2010;194(1):191–199.
- Martinsen AC, Sæther HK, Hol PK, Olsen DR, Skaane P. Iterative reconstruction reduces abdominal CT dose. *Eur J Radiol* 2012;81(7):1483–1487.
- Singh S, Kalra MK, Hsieh J, et al. Abdominal CT: comparison of adaptive statistical iterative and filtered back projection reconstruction techniques. *Radiology* 2010;257(2):373–383.
- Sagara Y, Hara AK, Pavlicek W, Silva AC, Paden RG, Wu Q. Abdominal CT: comparison of low-dose CT with adaptive statistical iterative reconstruction and routine-dose CT with filtered back projection in 53 patients. *AJR Am J Roentgenol* 2010;195(3):713–719.
- Prakash P, Kalra MK, Kambadakone AK, et al. Reducing abdominal CT radiation dose with adaptive statistical iterative reconstruction technique. *Invest Radiol* 2010;45(4):202–210.
- Mitsumori LM, Shuman WP, Busey JM, Kolokythas O, Koprowicz KM. Adaptive statistical iterative reconstruction versus filtered back projection in the same patient: 64 channel liver CT image quality and patient radiation dose. *Eur Radiol* 2012;22(1):138–143.
- Winklehner A, Karlo C, Puippe G, et al. Raw data-based iterative reconstruction in body CTA: evaluation of radiation dose saving potential. *Eur Radiol* 2011;21(12):2521–2526.
- Moscariello A, Takx RA, Schoepf UJ, et al. Coronary CT angiography: image quality, diagnostic accuracy, and potential for radiation dose reduction using a novel iterative image reconstruction technique-comparison with traditional filtered back projection. *Eur Radiol* 2011;21(10):2130–2138.
- Funama Y, Taguchi K, Utsunomiya D, et al. Combination of a low-tube-voltage technique with hybrid iterative reconstruction (iDose) algorithm at coronary computed tomographic angiography. *J Comput Assist Tomogr* 2011;35(4):480–485.
- Oda S, Utsunomiya D, Funama Y, et al. A hybrid iterative reconstruction algorithm that improves the image quality of low-tube-voltage coronary CT angiography. *AJR Am J Roentgenol* 2012;198(5):1126–1131.
- Noël PB, Fingerle AA, Renger B, Münzel D, Rummeny EJ, Dobritz M. Initial performance characterization of a clinical noise-suppressing reconstruction algorithm for MDCT. *AJR Am J Roentgenol* 2011;197(6):1404–1409.
- Miéville FA, Gudinchet F, Brunelle F, Bochud FO, Verdun FR. Iterative reconstruction methods in two different MDCT scanners: Physical metrics and 4-alternative forced-choice detectability experiments - A phantom approach. *Phys Med* 2012 Jan 2. [Epub ahead of print]
- Yu Z, Thibault JB, Bouman CA, Sauer KD, Hsieh J. Fast model-based X-ray CT reconstruction using spatially nonhomogeneous ICD optimization. *IEEE Trans Image Process* 2011;20(1):161–175.
- Suzuki S, Machida H, Tanaka I, Ueno E. Measurement of vascular wall attenuation: Comparison of CT angiography using model-based iterative reconstruction with standard filtered back-projection algorithm CT in vitro. *Eur J Radiol* 2012 Mar 19. [Epub ahead of print]
- Scheffel H, Stolzmann P, Schlett CL, et al. Coronary artery plaques: cardiac CT with model-based and adaptive-statistical iterative reconstruction technique. *Eur J Radiol* 2012;81(3):e363–e369.
- Mueck FG, Körner M, Scherr MK, et al. Upgrade to iterative image reconstruction (IR) in abdominal MDCT imaging: a clinical study for detailed parameter optimization beyond vendor recommendations using the adaptive statistical iterative reconstruction environment (ASIR). *Rof* 2012;184(3):229–238.
- Samei E, Badano A, Chakraborty D, et al. Assessment of display performance for medical imaging systems: executive summary of AAPM TG18 report. *Med Phys* 2005;32(4):1205–1225.
- Bongartz G, Golding SJ, Jurik AG, et al. European Guidelines of Quality Criteria in Computed Tomography. EUR 16252. <http://www.dr.s.dk/guidelines/ct/quality/htmlindex.htm>.
- Tapiovaara MJ, Sandborg M. How should low-contrast detail detectability be measured in fluoroscopy? *Med Phys* 2004;31(9):2564–2576.
- Barrett JF, Keat N. Artifacts in CT: recognition and avoidance. *RadioGraphics* 2004;24(6):1679–1691.
- Chen Y, Gao D, Nie C, et al. Bayesian statistical reconstruction for low-dose X-ray computed tomography using an adaptive-weighting nonlocal prior. *Comput Med Imaging Graph* 2009;33(7):495–500.